Balanced harvesting could reduce fisheries-induced evolution

Richard Law, Michael J. Plank

July 8, 2018

Alternative title: On fisheries-induced evolution under balanced harvesting

Running title: Selection and balanced harvesting

Richard Law: York Cross-Disciplinary Centre for Systems Analysis, Ron Cooke Hub, University of York, York YO10 5GE, UK.

richard.law@york.ac.uk

Michael J. Plank: School of Mathematics and Statistics and Te Pūnaha Matatini, University of Canterbury, Christchurch, New Zealand

Abstract

Current fisheries management pays little attention to fisheries-induced evolution. Methods of exploitation that have benefits in the short term, while ameliorating selection in the longer term would therefore be advantageous. Balanced harvesting is a potential candidate. This tries to bring fishing more in line with natural production, and some short-term benefits for conservation of aquatic ecosystems and for biomass yield have already been documented. It is also predicted to be relatively benign as a selective force on fish stocks, because it keeps the overall distribution of mortality relatively close to natural mortality.

We test this prediction, coupling an ecological model of marine, size-spectrum dynamics to an adaptive-dynamics model of life-history evolution. The evolutionary variable is the reproductive schedule, set by the maximum body mass and the mass at maturation. The prediction is supported by our numerical analysis: directional selection under balanced harvesting is approximately an order of magnitude weaker than in a standard fishery in which fish experience a fixed rate of fishing mortality after recruitment. The benefit of balanced harvesting follows from relatively little fishing on large fish, due to the low somatic production rates the big fish have. These results therefore support the general argument for protecting big, old fish, both for ecological and for evolutionary reasons. Slot fisheries that protect large fish share some qualitative features with balanced harvesting, and show similar evolutionary benefits.

Keywords: adaptive dynamics, ecosystem dynamics, fishing-induced selection, life-history evolution, production rate, size spectrum

Contents

1 Introduction

Fisheries are potentially important drivers of evolution in fish stocks, because fishing is often a major cause of mortality once fish reach a size at which they are harvested (Heino et al., 2015). There is good evidence for phenotypic change in wild populations consistent with expected effects of fishing, including the much-discussed case of maturation in North East Arctic cod (Eikeset et al., 2016; Enberg and Jørgensen, 2017). There is also experimental evidence that such evolution can take place (Haugen and Vøllestad, 2001; Conover and Munch, 2002; van Wijk et al., 2013). A molecular-genetic basis for such evolution, built on change in gene frequencies at loci linked to traits under selection in the wild, is also being developed (e.g. Chebib et al., 2016).

The precautionary principle calls for the minimization of risks from fisheries-induced evolution. We are the custodians of marine ecosystems, and responsible for leaving them undamaged for the future. This is enshrined in the Malawi Principle 5 of the Convention on Biological Diversity that motivates the ecosystem-based approach to fisheries management. However, despite the case for evolutionary impact assessment (Jørgensen et al., 2007), the day-to-day reality is that short-term issues of management supercede longer-term issues of fisheries-induced evolution (Law, 2007). An example is the plan of the European Union to eliminate discarding of species subject to quota or minimum landing-size regulations in European waters (Common Fisheries Policy reform EU Regulation 1380/2013). This is leading to the development of technical measures that will increase the selectivity of fishing, without consideration of the longer-term consequences for fisheries-induced evolution. The short-term solution comes potentially at the cost of exacerbating another, longer-term problem.

One way forward would be to develop methods of fishing that help in the immediate future and, at the same time, ameliorate selection in the longer term (Law, 2007). Balanced harvesting is a potential candidate for this. Balanced harvesting has been proposed as a way of exploiting fish stocks that would help to maintain the structure and functioning of marine ecosystems, by bringing fishing mortality more in line with the natural production of biomass by species and body sizes (Garcia et al., 2012). For clarity, we define balanced harvesting at the outset as setting fishing mortality rate to be proportional to the rate of somatic production (dimensions: mass vol.$^{-1}$ time^{-1}, or mass area^{-1} time^{-1}). Perfect balanced harvesting of an ecosystem is probably unachievable, but it does suggest a direction to go in. The bar for improvement appears to be low: no relationship could be found between fishing mortality rate and production rate of species in a recent study on the West of Scotland shelf ecosystem (Heath et al., 2017).

Matters could be improved both by a better balance of fishing mortality across species, and also by a better balance across body sizes within species. These paths towards a better balance are complementary, and both could bring fishing more in line with production rates. Both are the subject of research, including the distribution of fishing among species or functional groups (Garcia et al., 2012; Kolding et al., 2016a; Heath et al., 2017), and the distribution of fishing over body sizes (Law et al., 2012; Jacobsen et al., 2014; Kolding et al., 2016b; Law et al., 2016).

Several short-term benefits of balanced harvesting have been documented. The open-access fisheries on the Zambian side of Lake Kariba, with patterns of fishing mortality closer to balanced harvesting than the more regulated fisheries of Zimbabwe, give greater biomass yields with less impact on community structure (Kolding et al., 2016b). Reducing fishing mortality in species with low production rate helps to protect those that are rare and vulnerable (Law et al., 2016). It also reduces 'longevity overfishing', aiding the recovery of natural size structures, by allowing more survival of large individuals (Beamish et al., 2006). In this way, it improves the resilience of stocks to external perturbations (Hixon et al., 2014).

Here we consider a by-product of balanced harvesting, that could have longer-term benefits of slowing down fisheries-induced evolution. This is motivated by models that suggest balanced harvesting keeps total mortality within species closer to natural mortality than do traditional size-at-entry fisheries (Law et al., 2015, 2016). A better alignment between fishing mortality and natural mortality should reduce selection on the life-histories of fish stocks, and therefore reduce fisheries-induced evolution. This is primarily a prediction about the distribution of fishing mortality over body size within species, i.e. about balanced harvesting across body sizes within species, rather than across species. The purpose of this paper is to test this prediction, and the numerical results given here support it. In other words, balanced harvesting has an incidental, longer-term advantage of reducing directional selection from fishing, in addition to its short-term benefits on structure and functioning of marine ecosystems.

To do this work, we developed a method to connect the ecological dynamics of size spectra to a simple evolutionary model of adaptive dynamics (Kisdi and Geritz, 2010; Brännström et al., 2013). In technical terms, the work involves analysis of a transversal eigenvalue (the invasion fitness) of a high-dimensional Jacobian. The Jacobian can be resolved to a simple form that will allow broader study of evolution in complex, size-structured, marine ecosystems in the future.

2 Theory

The theory is built in three steps (Fig. 1). (Step 1) An ecological model of the dynamics of coupled size spectra: this is needed because there is no external notion of fitness in an adaptive-dynamics model—fitness of genetically distinct phenotypes emerges directly from the ecological processes. (Step 2) An evolutionary model based on adaptive dynamics, within which the ecological dynamics are nested: this moves an ancestral population through a sequence of mutation and selection events, driven by predation in the size spectra, leading eventually to a singular point at which there is no further evolution. The system is then at an evolutionarily stable state (ESS), before fishing is added. Without a separation of this kind, selection from fishing would be conflated with selection from predation taking place inside the food web. (Step 3) Calculation of the direction and strength of selection generated by a range of patterns of fishing at the ESS.

FIGURE 1 NEAR HERE

2.1 Ecological model

Dynamic size-spectrum models of marine ecosystems couple together an arbitrary number of species through size-dependent feeding (Andersen and Beyer, 2006; Hartvig et al., 2011; Blanchard et al., 2014; Jacobsen et al., 2014). Like any model of a complex, real-world marine ecosystems, they are a simplification. However, they are built up from realistic assumptions about the frequency of predator-prey interactions between individuals of a given size (Andersen et al., 2016). First, they assume that body size is the primary driver of the trophic level at which marine organisms feed. This property of marine trophic structure is in keeping with empirical research on stable isotopes of nitrogen (Jennings et al., 2001). Second, they deal explicitly with the growth of individuals as they eat other smaller organisms, so there is no external growth model, such as a von Bertalanffy growth equation. Third, they assume that the most common cause of death is through being eaten by larger organisms, which leaves less uncertainty about rates of natural mortality. Fourth, they assume that species are coupled through the body-size dependence of their prey: they are both predators on other species, and cannibals on themselves. Different species clearly can specialise in ways that affect their locations in food webs, and size-spectrum models incorporate some species-dependent feeding parameters. Importantly, unlike most models in fisheries science, size-spectrum models do the bookkeeping of biomass flowing in and out of species and size categories, as individuals eat one another and grow (e.g. Law et al.,

2016).

The state variables of size-spectrum models are functions that describe the density of organisms $\phi_i(w,t)$ as functions of body mass w and time t, where i is an index for species. The core of such a model is a system of partial differential equations, one equation for each species, describing how the density function $\phi_i(w,t)$ of each species unfolds over time through feeding (and consequent growth, reproduction and death). At their simplest, the partial differential equations take the form of a McKendrick—von Foerster equation, with body mass rather than age as the independent variable (Sinko and Streiffer, 1971; Silvert and Platt, 1978):

$$\frac{\partial}{\partial t}\phi_i = \overbrace{-\frac{\partial}{\partial w}\left[\tilde{g}_i\phi_i\right]}^{\text{(a)}} - \overbrace{\tilde{\mu}_{\text{tot},i}\phi_i}^{\text{(b)}}. \tag{2.1}$$

To help understand the right-hand side of this equation, Fig. 2 illustrates the meaning of terms (a) and (b). Term (a) describes the change in density at body mass w, due to feeding on smaller fish, contained in the function $\tilde{g}_i(w,t)$ the growth rate of individuals of body mass w at time t. This is calculated as a function of the abundance of smaller, conspecific and heterospecific individuals, of a suitable size to be prey of an individual of body mass w. Term (b) describes the change in density at body mass w, due to death; $\tilde{\mu}_{\text{tot},i}(w,t)$ is the total per capita death rate for individuals of body mass w. This is calculated as a function of the abundance of larger, conspecific and heterospecific individuals of a suitable size to be predators of an individual of body mass w at time t, plus other sources of mortality including sensesence and fishing. See Appendix A for full mathematical details.

FIGURE 2 NEAR HERE

In addition to species-dependent feeding, multispecies size spectra allow species to have different life histories. Life-history parameters include, for instance, the asymptotic body mass $w_{i,\infty}$, and body mass at 50 % maturation $w_{i,m}$. In non-seasonal, size-spectrum models, individuals allocate an increasing proportion of incoming biomass towards reproduction and away from somatic growth as they mature, the proportion reaching 1 at $w_{i,\infty}$ where somatic growth ends. For a given egg size, this is enough to define a schedule of reproduction at the level of species. Predation mortality and growth, which are also components of the life history, are not set as externalities in size-spectrum models, as they emerge from size- and density-dependent feeding in the food web. However, some additional death is incorporated, recognising that predation is not the only reason why organisms die, and such death may include mortality from fishing. In this way the life history is defined at the species level.

Note that the smallest organisms must have food to eat if they are to grow, so size spectra have to be extended down into the spectrum of unicellular plankton. For simplicity, we used a fixed plankton spectrum, set to values that correspond approximately to those observed. This is equivalent to an assumption that the plankton dynamics happen on a faster timescale and cannot be exhausted by predation, and it has the effect that fish population growth is not limited by the plankton. However, the predation and cannibalism among the fish are enough to hold their population growth in check, as long as the upper limit of plankton body size is kept sufficiently small relative to the sizes of maturation of the fish species.

2.2 Evolutionary model

We used adaptive dynamics to describe phenotypic evolution. The theory of adaptive dynamics was developed in the 1990s to provide a direct link between population dynamics and phenotypic evolution (Kisdi and Geritz, 2010). The basic dynamics and their graphical representation were given in some early papers (Metz et al., 1992; Dieckmann and Law, 1996; Metz et al., 1996; Geritz et al., 1998), and a review by Brännström et al. (2013) gives an overview of the subject. The idea is that phenotypic traits, such as asymptotic body mass $w_{i,\infty}$, although fixed in ecological time, have a genetic component that is under selection driven directly by the ecological processes. In the context of multispecies size spectra, adaptive dynamics allows evolution of traits to emerge from natural selection generated by the multispecies food web without simplifying the ecology. There is a cost to this in terms of certain assumptions, the most important being a time-scale separation between the ecological and evolutionary dynamics: mutations to the trait have to be infrequent enough for the food web to be at its asymptotic state (typically an equilibrium point) before the next mutant appears. Other assumptions to make the dynamics more tractable include small mutational steps, a simple asexual mutation-selection process (a trait-substitution sequence), and populations that are dominated by a single phenotype at each step.

The path of evolution is determined by the initial rate of increase (invasion fitness) of mutants as they arise in the resident food web. An evolutionary step starts with the ecological system running to its asymptotic state with a set of resident trait values $\mathbf{s}$ for the species. Having reached this state, a function $\lambda_i(s_i', \mathbf{s})$ defines the invasion fitness of a mutant with an altered trait value s_i' in species i. Despite the complexity of the resident food web, the eigenvalue corresponding to the invasion fitness is found relatively easily from a Jacobian matrix that contains the mutant dynamics Eq. (B.1) (Appendix B). Evolution of the set of traits is then given by a

system of canonical equations, with one equation for each evolving species:

$$\frac{ds_i}{dt} = k_i \frac{\partial}{\partial s_i'} \lambda_i(s_i', \mathbf{s})\big|_{s_i'=s_i} \tag{2.2}$$

(Dieckmann and Law, 1996), where k_i is an evolutionary rate constant for species i. The core information about selection is carried by the partial derivative of the invasion fitness in the direction of the mutant when the mutant is rare (the selection gradient). What happens if the mutant increases would seem to be left unanswered by this, but a theorem gives the conditions under which invasion implies fixation of the mutant, and these conditions apply quite widely (Geritz et al., 2002).

2.3 Strength of directional selection from fishing

To examine some basic effects of selective fishing we took just two interacting fish species from the general framework above, and allowed evolution of one trait on one of them. The evolving trait was the asymptotic body mass w_∞, and the mass at 50 % maturation w_m was assumed to be a fixed proportion of this, so that the whole reproductive schedule would move with body size as the trait evolved. This is in keeping with the similar length ratios l_m/l_∞ observed (a) in similar-shaped fish species, (b) in taxonomically related fish species, and (c) in different populations of single species, despite substantial variation in l_∞ (Beverton, 1992; Froese and Binohlan, 2000). (As only one species is evolving, the species index is omitted below.)

In an evolving system as simple as this, the invasion-fitness surface $\lambda(w_\infty', w_\infty)$ is enough to show the qualitative outcome of evolution. An example is given in Fig. 3: the surface is saddle-like, and has a singular point of evolution w_∞^* at which the selection gradient in Eq. (2.2) is zero. The singular point can be seen by taking a section through through the surface at $\lambda = 0$ known as the pairwise invasibility plot (PIP) (Fig. 3); the singular point is at the intersection of the two lines (Geritz et al., 1998; Brännström et al., 2013). In the system described below, the asymptotic mass evolved to this point and came to rest there. Thus, in this instance, the singular point is a continuously stable strategy (CSS), i.e. an evolutionarily stable strategy (ESS) (Maynard Smith and Price, 1973), to which there is convergence through evolution (Geritz et al., 1998; Brännström et al., 2013). We take w_∞^* as the trait value of the evolved ancestral population, prior to the introduction of fishing.

FIGURE 3 NEAR HERE

When fishing mortality is added, the shape of the invasion-fitness surface is distorted, and the singular point at w_∞^* becomes invadable by mutants.

Some examples are shown in Fig. 4a. The gradient at w_∞^* clearly depends on the fishing mortality, and shows the strength of selection generated by fishing. Thus we measure the strength of directional selection S as the slope at the singular point w_∞^*:

$$S = \frac{\partial}{\partial \log w'_\infty} \lambda(w'_\infty, w_\infty)\big|_{w'_\infty = w_\infty^*}, \tag{2.3}$$

to compare the selective effects of different patterns of exploitation below, as shown in the inset of Fig. 4a. (Fig. 3 shows the direction along which the slope is measured.) If the slope becomes negative when fishing is introduced, mutants with smaller w_∞ can invade, and those with larger w_∞ cannot; steeper this slope, the greater the selective advantage of these mutants.

In due course, a new mortality regime would cause evolution to another phenotypic state. However, it would be inadvisable to use a simple adaptive-dynamics model to investigate this. The strong selection generated by fishing would violate the time-scale separation between ecological and evolutionary dynamics assumed in the adaptive-dynamics model. Other methods avoiding this assumption would be preferred, such as quantitative-genetic and ecogenetic models (Andersen and Brander, 2009; Dunlop et al., 2009). Adaptive dynamics is used in this paper just to construct an ancestral singular point of evolution, and to measure the strength of selection generated by patterns of fishing mortality at that singular point.

FIGURE 4 NEAR HERE

3 Numerical results

3.1 Ancestral singular point of evolution

For numerical analysis, we took an ecological system similar to that of Law et al. (2016), comprising a fixed plankton spectrum, together with two fish species, one growing to a small size, and the other to a large size (notionally Atlantic mackerel *Scomber scombrus*, Scombridae, and Atlantic cod *Gadus morhua*, Gadidae). The parameter values specifying the ecological system are given in Appendix C. Some effects of different fishing regimes on this and simpler systems in the absence of evolution have been shown in earlier papers (Law et al., 2015, 2016), but an evolutionary model is needed to examine the strength of selection generated by different fishing methods.

Cod was taken as the evolving species, and the evolving trait was w_∞ with the 50 % maturation as a fixed proportion, 1/15 of w_∞. A singular

point of evolution of the ancestral cod was found at $w^*_\infty \approx 85$ kg (Fig. 3), near the size of the largest cod ever recorded (Kolding personal communication). Equivalently, mass at 50 % maturity w^*_m was 5.67 kg. Predation by mackerel on small cod was the main driver of late maturation in cod in our numerical model, and the strength of predation was therefore tuned to obtain the ancestral value (Appendix C). (In the absence of mackerel, evolution of the ancestral cod would bring cod to a singular point of evolution at $w^*_\infty = 27$ kg in our numerical analysis (results not shown).) The large asymptotic mass and longevity of ancestral cod can be interpreted as an evolutionary outcome of the escape that this gives from heavy predation early in life (Williams, 1966, p.89-91).

The invulnerability of the ancestral cod at $w^*_\infty \approx 85$ kg in the absence of fishing is evident from the section through the invasion-fitness surface in the direction of the mutant at w^*_∞ (Fig. 4a, heavy dotted curve). This line reaches its maximum value of zero at w^*_∞: in other words, w^*_∞ is an ESS, uninvadable by any mutant with another trait value w'_∞ in its neighbourhood. The point w^*_∞ is taken as the state to which cod evolved prior to the introduction of fishing.

3.2 Patterns of fishing mortality

We considered three ways in which to distribute fishing mortality rate over body size (Fig. 5). (1) Balanced harvesting sets the rate to be proportional to the current rate of somatic production at each size, from some minimum size of capture onwards (see Appendix D). (2) Size-at-entry fishing has a minimum capture size above which the fishing mortality is constant irrespective of body size. (3) Slot fishing has constant fishing mortality like size-at-entry, but has an additional maximum body size above which fish are not caught. Each fishing pattern has a parameter controlling the overall intensity of fishing. Under size-at-entry and slot fishing, this is the fishing mortality rate, F, within the exploited size range. Under balanced harvesting, no single value of F can be used, because F is a function of body size. Instead, the constant of proportionality c (units: $\mathrm{m}^3\ \mathrm{g}^{-1}$) between the production rate and fishing mortality, is taken as the parameter (Appendix D).

FIGURE 5 NEAR HERE

Thus the fishing patterns differ in the fishing mortality above some minimum size of capture (assumed to be knife-edge). Notice that the fall in somatic growth rate and biomass, which typically happens when fish become large for their species, has the effect of making the somatic production rate

decrease. This is therefore accompanied by a corresponding fall in fishing mortality under balanced harvesting. The different fishing patterns distort the invasion-fitness surface (Fig. 3) in different ways, generating different selection gradients, which will be described below.

The key to understanding the selection on cod generated by fishing is through the changing regime of mortality on cod that fishing brings about. This comes in two parts. First, there is a direct effect on mortality from the fish that are caught. Second, hidden beneath this, are changes in intrinsic mortality, predation mortality and cannibalism inside the size-structured food web, as it adjusts to the fishing. The ecological size-spectrum dynamics automatically keep track of these internal changes, and the effects of the changes are felt by non-target as well as by target species.

3.3 Mortality from mackerel predation

The hidden effects of predation are important. For instance, mackerel is not a passive partner in the evolution of cod: predation by mackerel is part of the mortality experienced by cod. If mackerel are harvested, the predation by mackerel on cod is reduced, and this leaves a footprint on the invasion fitness of mutants w'_∞ in cod, favouring those with lower w'_∞ (Fig. 4a, dash-dot line), irrespective of any fishing on cod.

We assumed a fixed background of fishing on mackerel, harvested as a size-at-entry fishery with a fishing mortality rate 0.5 yr^{-1} starting at a body mass 250 g. We did this because cod could be seriously depleted by the combined effects of heavy fishing and predation from mackerel, if the latter was unexploited. So fishing on mackerel here was taken as a fixed part of the environment of cod, and was not balanced to match fishing on cod (cf. Law et al., 2016). The selection gradients on cod under fishing should therefore be taken relative to the selection gradient on cod already caused by catching mackerel. However, the impact on cod of fishing mackerel at this level is relatively small, as shown in Fig. 4a.

3.4 Selection in balanced and size-at-entry fisheries

A balanced fishery on cod leads to much less selection on the life history than a size-at-entry fishery (Fig. 4a: continuous and dashed lines). This can be seen from the much steeper gradient of the invasion fitness under size-at-entry (continuous curve) than under balanced harvesting (dashed curve), and is consistent with the prediction that balanced harvesting is relatively benign in its effects on fisheries-induced evolution. Depending

on whether the selective effect of fishing mackerel is allowed for, the selection gradient in the size-at-entry fishery is from about five to twenty times that in the balanced fishery at the same biomass yield. Fig. 4b extends the comparison of balanced and size-at-entry fisheries to show the relation between selection gradient and biomass yield as cod fishing mortality increases from zero (the fishing mortality rate on mackerel is fixed throughout). The major benefits from balanced harvesting in reducing selection are clear. Note that the selection gradient on cod is negative even when there is no fishing on cod, because mackerel fishing automatically changes the pattern of predation on cod.

Fig. 6 gives a sensitivity analysis of the effect of varying fishing pressure over a range of minimum capture sizes. This confirms the much weaker selection in balanced than in size-at-entry fisheries, as the minimum capture size is varied: for a given biomass yield, the selection gradient is substantially closer to zero in balanced than in size-at-entry fishing. Yield rises to a peak as fishing increases and then falls until extinction occurs. Balanced harvesting gives the greatest benefits to reducing selection with moderate levels of fishing, well before the maximum yield is reached. The yield does not return smoothly to zero as fishing increases; instead there is a threshold when the combined effects of fishing, cannabilism, and predation by mackerel reach a point at which cod collapses.

FIGURE 6 NEAR HERE

The main benefit of balanced harvesting comes from bringing fishing in line with production rates of large (not small) fish. This is evident from the fact that the minimum capture sizes in the balanced fisheries have relatively little effect on the selection gradients as the biomass yield is growing (Fig. 6a). In contrast, in the size-at-entry fisheries, selection for earlier maturation becomes stronger (i.e., S becomes more negative), as fishing becomes more concentrated on adults (Fig. 6b). In the balanced fisheries, the selection gradients in fact get slightly closer to zero as the minimum capture size increases (Fig. 6a), thereby countering the effect of mackerel fishing.

3.5 Selection in slot fisheries

A detailed balancing of fishing to production rate by species and body size would be hard to achieve in practice. Evidently, low fishing mortality on the big fish that have low production rates is the key to reducing fisheries-induced selection on the reproduction schedule. We therefore examined the sensitivity of selection to a range of slot fisheries, as a first approximation to

balanced harvesting (Fig. 7), using two fixed ratios of maximum/minimum capture size of 5 and 10. Like balanced and size-at-entry fisheries, the yield rises to a peak as fishing increases. But unlike balanced harvesting, the extinction point under fishing can be close to the peak unless the mininum capture size is large. Since collapse could occur with little warning, slot fisheries on small fish would need to be implemented with care.

FIGURE 7 NEAR HERE

The effect of sliding the slot fisheries across the life history of cod is consistent with a basic notion of life-history theory, that organisms evolve to avoid states where they are at their most vulnerable (Williams, 1966). When small cod are caught (minimum capture sizes: 30, 100, 300 g), the ancestral advantage in large body size as an escape from predation weakens and, as in balanced harvesting, relatively weak selection for earlier maturation occurs. Such fishing is undoing part of the ancestral selection pressure for late maturation. When intermediate-sized cod are caught (minimum capture size: 1 kg), delayed maturation allows faster growth through the vulnerable size range, pushing the selection gradient a little in the opposite direction, even to the point of reversing the direction of selection (Fig. 7b). When large cod are caught (minimum capture size: 3 kg), delaying maturation carries the heavy cost of potentially not reproducing at all, and, as in size-at-entry fishing, there is strong selection for early maturation.

The reversal of fisheries-induced selection is remarkable (Fig. 7b, fishing from 1 to 10 kg). We interpret it in part as an interaction with the mackerel fishery, since this slot size range would include cod that would otherwise be eating the exploited size range of mackerel to a major degree. Catching these cod thus allows more of these mackerel to escape predation, despite the fishery on them (and also more escape from predation by cod of a similar size). The outcome is heavier predation on cod still earlier in life, and overall selection for later maturation.

4 Discussion

Our results support the prediction that balanced harvesting is a good deal more benign than traditional size-at-entry fisheries, as a selective pressure on the life histories of fish. This is contingent on fishing mortality being set at a moderate level. Although the ecological context of multispecies size spectra is different from previous work, the basic feature, that organisms evolve not to linger in vulnerable states, is congruent with earlier work on life-history evolution (Williams, 1966; Edley and Law, 1988), suggesting a robustness of the results that goes beyond particular model structures.

The simple message is that, to keep fishing-induced selection small, it helps to protect big fish with low production rates.

Importantly, balanced harvesting is as much about *reducing* fishing on components of ecosystems that have low production, as it is about fishing on those that have high production. Fish that are big for their species typically have relatively low somatic production rates, (a) because they have low mass-specific somatic growth rates, and (b) because a history of fishing tends to truncate size structures, leaving the remaining big fish with low biomass densities. The somatic production rate is simply the product (a) $\times$ (b), and balanced harvesting therefore calls for correspondingly little fishing on these big fish. Balanced harvesting thus aligns with a major stream of thinking that big, old fish need protection both for ecological and for evolutionary reasons (Beamish et al., 2006; Hsieh et al., 2006, 2010; Hixon et al., 2014). Balanced harvesting contributes to this literature in suggesting somatic production rate as a quantitative guide for setting relative levels of fishing mortality.

A precise balancing of fishing mortality to production rate by body size would be hard to achieve in practice. Slot fisheries that select an intermediate range of body size resemble balanced harvesting at a qualitative level, as they create a refuge for large fish. Our results on fisheries-induced selection caused by slot fishing are consistent with those of a recent study on the use of gillnets in NE Arctic cod (Zimmermann and Jørgensen, 2017). Slot fishing deserves attention in the drive for increased selectivity to reduce discarding (Common Fisheries Policy reform EU Regulation 1380/2013). Selectivity *per se* is not the issue—it is what is being selected that matters. To get the evolutionary benefits from slot fisheries, their upper limits should not extend too far into adult life, as that would generate a strong selective advantage for early reproduction. Slot fisheries involving juveniles have to be implemented with caution because of the clear danger that stocks could collapse from over-exploitation.

Taking a multispecies, size-spectrum model as the ecological input into a model of adaptive dynamics, provides a new route into life-history evolution in general, and fisheries-induced evolution in particular. It deals internally with all the density-dependent growth and mortality generated by predation and cannibalism in the size-structured, food-web model. In this way, it removes an artificial separation of natural mortality from fishing mortality. This has some interesting consequences. For instance, it shows how fishing on one species generates selection on another (unexploited) species, as the food web adjusts to the fishing. It also shows that a fishing regime, appropriately chosen, could change the predation mortality generated within the food-web, reversing the direction of selection caused by fishing. This

would be system specific, and would require a detailed understanding of how the food web works. The framework we have developed offers a route to exploring the selection pressures generated by fishing on multiple species within a marine ecosystem.

Quite apart from the context of fisheries-induced evolution, coupling size-spectrum dynamics to adaptive dynamics should facilitate research into broader issues about evolution in aquatic food webs. Current models of size spectrum dynamics contain a number of parameters that could be evolutionary variables, such as how far down the food web predators are feeding, how broad their diets are, and how active they are. Further ecological parameters are likely to become part of the language of size-spectrum models as the research field develops, and adaptive dynamics provides a flexible framework for studying their evolution.

One general evolutionary issue is whether there is a simple maximisation principle at work. Such a principle, that species evolve to reproduce at the body size at which cohort biomass is greatest, has been been suggested by Froese et al. (2016) as an argument for the implausability of peaks in biomass at small body size (Law et al., 2016). Our evolutionary analysis does not support this maximum-biomass principle: irrespective of biomass peaks, predation by mackerel on small cod generates an advantage for late maturation in cod. Peaks and troughs in cohort biomass (and equivalently somatic production rate) occur at body sizes where mass-specific growth rate and death rate intersect (Law et al., 2016, Appendix E). These rate functions are nonlinear and rather labile as they are strongly affected by the prevailing predation in the food web. We would therefore expect the peaks of cohort biomass to move around during the course of evolution. Until more is known about such evolution, it is probably sensible to keep an open mind about where peaks in cohort biomass are located with respect to body size, and to try to understand more about the location of peaks from empirical work.

Among the caveats about this study is the reduction of the life history to a single scalar measure of reproduction, to allow the whole reproduction schedule to shift to smaller or larger body sizes. This allows some basic calculations, but it simplifies the multidimensional, phenotypic structure of the life history. For instance, there is special interest in probabilistic maturation reaction norms (PMRNs) as sensitive indicators of fisheries-induced evolution (Heino et al., 2002; Heino and Dieckmann, 2008). The ecological, size-spectrum dynamics do carry dependence of growth on food, so there is an implied PMRN, which would be seen as prey densities change; this PMRN would depend on age (not body size) with the size-spectrum model as implemented here.

A second caveat is that we have not dealt with the rate at which fisheries-induced evolution takes place. This is because it would be hard to justify adaptive-dynamics' time-scale separation between ecological and evolutionary dynamics in contemporary fisheries. Our results say only that, for a given biomass yield, the strength of selection could be brought down by roughly an order of magnitude by moving from size-at-entry fishing to balanced and appropriate slot fisheries. The rate of evolutionary change caused by fishing is widely discussed (e.g. Jørgensen et al., 2007; Andersen and Brander, 2009; Audzijonyte et al., 2013a; Heino et al., 2015), but has not gained traction in the practical management of fisheries. This is unfortunate because the longer, decadal time-scale of fisheries-induced evolution does not absolve managers of marine ecosystems from responsibility for such changes. One reason for linking fisheries-induced evolution to balanced harvesting is that, as well as helping to resolve some short-term issues, it can evidently also assist conservation of fish stocks in the longer term.

A third caveat is that fishing gear obviously has many selective effects other than changing the mortality rate, for instance on behaviour or reproductive phenology (Heino et al., 2015; Andersen et al., 2018; Tillotson and Quinn, 2018). Such selective effects of fishing gear can be quite different from those generated by natural predators. The prediction in this paper is simply about the distribution of mortality on the evolution of life histories under different schemes of fishing.

Our main result, that fisheries-induced selection would be reduced by lowering fishing mortality on fish that are big for their species, should be robust. However the fine details of feedbacks within food webs are bound to be context dependent. Feedbacks in multispecies, size-structured food webs are intricate, and the challenge as fisheries science moves towards an ecosystem approach is to see what, if any, broad robust patterns emerge from the fine details (Audzijonyte et al., 2013b).

Acknowledgements

This research received funding from the European Commissions Horizon 2020 Research and Innovation Programme under Grant Agreement No. 634495 for the project Science, Technology, and Society Initiative to minimize Unwanted Catches in European Fisheries (MINOUW). MJP was partly funded by Te Pūnaha Matatini, a New Zealand Centre of Research Excellence. The work was facilitated by the School of Mathematics and Statistics, University of Canterbury, New Zealand, which hosted a research

visit by RL. Gustav Delius and Richard Southwell gave advice on implementing the fast Fourier transform.

References

Andersen, K. H. and Beyer, J. E. (2006). Asymptotic size determines species abundance in the marine size spectrum. *American Naturalist*, 168:54–61.

Andersen, K. H., Blanchard, J. L., Fulton, E. A., Gislason, H., Jacobsen, N. S., and van Kooten, T. (2016). Assumptions behind size-based ecosystem models are realistic. *ICES Journal of Marine Science*, 73:1651–1655. doi:10.1093/icesjms/fsv211.

Andersen, K. H. and Brander, K. (2009). Expected rate of fisheries-induced evolution is slow. *Proceedings of the National Academy of Sciences USA*, 106:11657–11660. doi:10.1073pnas.0901690106.

Andersen, K. H., Marty, L., and Arlinghaus, R. (2018). Evolution of boldness and life history in response to selective harvesting. *Canadian Journal of Fisheries and Aquatic Sciences*, 75:271–281. dx.doi.org/10.1139/cjfas–2016–0350.

Audzijonyte, A., Kuparinen, A., and Fulton, E. A. (2013a). How fast is fisheries-induced evolution? quantitative analysis of modelling and empirical studies. *Evolutionary Applications*, 6:585–595. doi:10.1111/eva.12044.

Audzijonyte, A., Kuparinen, A., Gorton, R., and Fulton, E. A. (2013b). Ecological consequences of body size decline in harvested fish species: positive feedback loops in trophic interactions amplify human impact. *Biology Letters*, 9:20121103. doi:10.1098/rsbl.2012.1103.

Beamish, R. J., McFarlane, G. A., and Benson, A. (2006). Longevity overfishing. *Progress in Oceanography*, 68:289–302. doi:10.1016/j.pocean.2006.02.005.

Beverton, R. J. H. (1992). Patterns of reproductive strategy parameters in some marine teleost fishes. *Journal of Fish Biology*, 41 (Supplement B):137–160. doi.org/10.1111/j.1095–8649.1992.tb03875.x.

Blanchard, J. L., Andersen, K. H., Scott, F., Hintzen, N. T., Piet, G., and Jennings, S. (2014). Evaluating targets and trade-offs among fisheries and conservation objectives using a multispecies size spectrum model. *Journal of Applied Ecology*, 51:612–622. doi:10.1111/1365–2664.12238.

Brännström, Å., Johansson, J., and von Festenberg, N. (2013). The hitchhikers guide to adaptive dynamics. *Games*, 4:304–328. doi:10.3390/g4030304.

Chebib, J., Renaut, S., Bernatchez, L., and Rogers, S. M. (2016). Genetic structure and within-generation genome scan analysis of fisheries-induced evolution in a lake whitefish (*Coregonus clupeaformis*) population. *Conservation Genetics*, 17:473–483. doi:10.1007/s10592–015–0797–y.

Conover, D. O. and Munch, S. B. (2002). Sustaining fisheries yields over evolutionary time scales. *Science*, 297:94–96.

Datta, S., Delius, G. W., and Law, R. (2010). A jump-growth model for predator-prey dynamics: derivation and application to marine ecosystems. *Bulletin of Mathematical Biology*, 72:1361–1382. doi:10.1007/s11538–009–9496–5.

Datta, S., Delius, G. W., Law, R., and Plank, M. J. (2011). A stability analysis of the power-law steady state of marine size spectra. *Journal of Mathematical Biology*, 63:779–799. doi:10.1007/s00285–010–0387–z.

Dieckmann, U. and Law, R. (1996). The dynamical theory of coevolution: a derivation from stochastic ecological processes. *Journal of Mathematical Biology*, 34:579–612.

Dunlop, E. S., Heino, M., and Dieckmann, U. (2009). Eco-genetic modeling of contemporary life-history evolution. *Ecological Applications*, 19:1815–1834.

Edley, M. T. and Law, R. (1988). Evolution of life histories and yields in experimental populations of *Daphnia magna*. *Biological Journal of the Linnean Society*, 34:309–326.

Eikeset, A. M., Dunlop, E. S., Heino, M., Storvik, G., Stenseth, N. C., and Dieckmann, U. (2016). Roles of density-dependent growth and life history evolution in accounting for fisheries-induced trait changes. *Proceedings of the National Academy of Sciences USA*, 113:15030–15035. doi:10.1073/pnas.1525749113.

Enberg, K. and Jørgensen, C. (2017). Conclusion that fishing-induced evolution is negligible follows from model assumptions. *Proceedings of the National Academy of Sciences USA*, 114:. doi:10.1073/pnas.1700708114.

Froese, R. and Binohlan, C. (2000). Empirical relationships to estimate asymptotic length, length at first maturity and length at maximum yield per recruit in fishes, with a simple method to evaluate length frequency data. *Journal of Fish Biology*, 56:758–773. doi:10.1006/jfbi.1999.1194.

Froese, R., Walters, C., Pauly, D., Winker, H., Weyl, O. L. F., Demirel, N., Tsikliras, A. C., and Holt, S. J. (2016). A critique of the balanced harvesting approach to fishing. *ICES Journal of Marine Science*, 73:1640–1650. doi:10.1093/icesjms/fsv122.

Garcia, S. M., Kolding, J., Rice, J., Rochet, M.-J., Zhou, S., Arimoto, T., Beyer, J. E., Borges, L., Bundy, A., Dunn, D., Graham, N., Hall, M., Heino, M., Law, R., Makino, M., Rijnsdorp, A. D., Simard, F., and Smith, A. D. M. (2012). Reconsidering the consequences of selective fisheries. *Science*, 335:1045–1047.

Geritz, S. A. H., Gyllenberg, M., Jacobs, F. J. A., and Parvinen, K. (2002). Invasion dynamics and attractor inheritance. *Journal of Mathematical Biology*, 44:560–560. doi:10.1007/s002850100136.

Geritz, S. A. H., Kisdi, É., Meszéna, G., and Metz, J. A. J. (1998). Evolutionarily singular strategies and the adaptive growth and branching of the evolutionary tree. *Evolutionary Ecology*, 12:35–57.

Hartvig, M., Andersen, K. H., and Beyer, J. E. (2011). Food web framework for size-structured populations. *Journal of Theoretical Biology*, 272:113–122. doi:10.1016/j.jtbi.2010.12.006.

Haugen, T. O. and Vøllestad, L. A. (2001). A century of life-history evolution in grayling. *Genetica*, 112113:475–491.

Heath, M., Law, R., and Searle, K. (2017). Scoping the background information for an ecosystem approach to fisheries in scottish waters: Review of predator-prey interactions with fisheries, and balanced harvesting. Technical report, A study commissioned by Fisheries Innovation Scotland (FIS). ISBN: 978-1-911123-10-1, www.fiscot.org.

Heino, M. and Dieckmann, U. (2008). Detecting fisheries-induced life-history evolution: an overview of the reaction norm approach. *Bulletin of Marine Science*, 83:69–93.

Heino, M., Dieckmann, U., and Godø, O. R. (2002). Measuring probabilistic reaction norms for age and size at maturation. *Evolution*, 56:669–678.

Heino, M., Pauli, B. D., and Dieckmann, U. (2015). Fisheries-induced evolution. *Annual Review of Ecology and Systematics*, 46:461–480. doi:10.1146/annurev–ecolsys–112414–054339.

Hixon, M. A., Johnson, D. W., and Sogard, S. M. (2014). BOFFFFs: on the importance of conserving old-growth age structure in fishery populations. *ICES Journal of Marine Science*, 73:1623–1631. doi:10.1093/icesjms/fst200.

649 Hsieh, C.-H., Reiss, C. S., Hunter, J. R., Beddington, J. R., May, R. M.,
650 and Sugihara, G. (2006). Fishing elevates variability in the abundance
651 of exploited species. *Nature*, 443:859–862. doi:10.1038/nature05232.

652 Hsieh, C.-h., Yamauchi, A., Nakazawa, T., and Wang, W.-F. (2010). Fish-
653 ing effects on age and spatial structures undermine population stability
654 of fishes. *Aquatic Sciences*, 72:165–178. doi:10.1007/s00027–009–0122–2.

655 Jacobsen, N. S., Gislason, H., and Andersen, K. H. (2014). The conse-
656 quences of balanced harvesting of fish communities. *Proceedings of the*
657 *Royal Society B*, 281:20132701. doi:0.1098/rspb.2013.2701.

658 Jennings, S., Pinnegar, J. K., Polunin, N. V. C., and Boon, T. W. (2001).
659 Weak cross-species relationships between body size and trophic level belie
660 powerful size-based trophic structuring in fish communities. *Journal of*
661 *Animal Ecology*, 70:934–944.

662 Jørgensen, C., Enberg, K., Dunlop, E. S., Arlinghaus, R., Boukal, D. S.,
663 Brander, K., Ernande, B., Gårdmark, A., Johnston, F., Matsumura, S.,
664 Pardoe, H., Raab, K., Silva, A., Vainikka, A., Dieckmann, U., Heino, M.,
665 and Rijnsdorp, A. D. (2007). Managing evolving fish stocks. *Science*,
666 318:1247–1248. doi:10.1126/science.1148089.

667 Kisdi, É. and Geritz, S. A. H. (2010). Adaptive dynamics: a framework
668 to model evolution in the ecological theatre. *Journal of Mathematical*
669 *Biology*, 61:165–169. doi:10.1007/s00285–009–0300–9.

670 Kolding, J., Bundy, A., van Zwieten, P. A. M., and Plank, M. J. (2016a).
671 Fisheries, the inverted food pyramid. *ICES Journal of Marine Science*,
672 73:1697–1713. doi:10.1093/icesjms/fsv225.

673 Kolding, J., Jacobsen, N. S., Andersen, K. H., and van Zwieten, P. A. M.
674 (2016b). Maximizing fisheries yields while maintaining community struc-
675 ture. *Canadian Journal of Fisheries and Aquatic Sciences*, 73:644–655.
676 doi:10.1139/cjfas–2015–0098.

677 Law, R. (2007). Fisheries-induced evolution: present status and future
678 directions. *Marine Ecology Progress Series*, 335:271–277.

679 Law, R., Kolding, J., and Plank, M. J. (2015). Squaring the circle: recon-
680 ciling fishing and conservation of aquatic ecosystems. *Fish and Fisheries*,
681 16:160–174. doi:10.1111/faf.12056.

682 Law, R., Plank, M. J., and Kolding, J. (2012). On balanced exploitation
683 of marine ecosystems: results from dynamic size spectra. *ICES Journal*
684 *of Marine Science*, 69:602–614. doi:10.1093/icesjms/fss031.

Law, R., Plank, M. J., and Kolding, J. (2016). Balanced exploitation and coexistence of interacting, size-structured, fish species. *Fish and Fisheries*, 17:281–302. doi:10.1111/faf.12098.

Maynard Smith, J. and Price, G. R. (1973). The logic of animal conflict. *Nature*, 246:15–18.

Metz, J. A. J., Geritz, S. A. H., Meszéna, G., Jacobs, F. J. A., and van Heerwaarden, J. S. (1996). Adaptive dynamics, a geometrical study of the consequences of nearly faithful reproduction. In van Strien, S. J. and Verduyn Lunel, S. M., editors, *Stochastic and Spatial Structures of Dynamical Systems*, pages 183–231. North-Holland Publishing Co, Amsterdam, The Netherlands.

Metz, J. A. J., Nisbet, R. M., and Geritz, S. A. H. (1992). How should we define fitness for general ecological scenarios? *Trends in Ecology and Evoution*, 7:198–202. doi.org/10.1016/0169–5347(92)90073–K.

Silvert, W. and Platt, T. (1978). Energy flux in the pelagic ecosystem: a time-dependent equation. *Limnology and Oceanography*, 23:813–816.

Sinko, J. W. and Streiffer, W. (1971). A model for populations reproducing by fission. *Ecology*, 52:330–335.

Tillotson, M. D. and Quinn, T. P. (2018). Selection on the timing of migration and breeding: a neglected aspect of fishing-induced evolution and trait change. *Fish and Fisheries*, 19:170–181. doi:10.1111/faf.12248.

van Wijk, S. J., Taylor, M. I., Creer, S., Dreyer, C., Rodrigues, F. M., Ramnarine, I. W., van Oosterhout, C., and Carvalho, G. R. (2013). Experimental harvesting of fish populations drives genetically based shifts in body size and maturation. *Frontiers in Ecology and the Environment*, 11:181–187. doi:10.1890/120229.

Williams, G. C. (1966). *Adaptation and Natural Selection*. Princeton University Press Princeton.

Zimmermann, F. and Jørgensen, C. (2017). Taking animal breeding into the wild: regulation of fishing gear can make fish stocks evolve higher productivity. *Marine Ecology Progress series*, 563:185–195. doi:10.3354/meps11996.

Tables

Table 1: Model parameters and values.

Parameter	Mackerel	Cod	Unit	Comments
				Fish life histories:
$w_0 e^{x_{i,0}}$	0.001	0.001	g	mass of fish egg
$w_0 e^{x_{i,m}}$	200	evolving	g	mass at 50% maturity
$w_0 e^{x_{i,\infty}}$	650	evolving	g	asymptotic mass
$\rho_{i,m}$	15	8	–	controls the body-size range over which maturation occurs
ρ	0.2	0.2	–	exponent for approach to asymptotic body size in reproduction funcion
				Dynamic size spectra of fish species:
K	0.2	0.2	–	food conversion efficiency
α_i	0.8	0.8	–	search rate scaling exponent
A_i	750	700	$\mathrm{m}^3\ \mathrm{yr}^{-1}\ \mathrm{g}^{-\alpha}$	feeding rate constant
β_i	6	4.5	–	natural log of mean predator prey mass ratio
σ_i	2.5	1.9	–	diet breadth
$\mu_{o,i}^{(0)}$	0.1	0.1	yr^{-1}	intrinsic mortality rate at birth
ξ	-0.15	-0.15	–	exponent for intrinsic mortality
				Fixed plankton size spectrum:
$w_0 e^{x_{0,min}}$	4.8×10^{-11}		g	lowest body mass of plankton
$w_0 e^{x_{0,max}}$	0.03		g	greatest body mass of plankton
$u_{0,0}$	100		m^{-3}	plankton density at 1 mg
γ	2		–	exponent of plankton spectrum

Figure legends

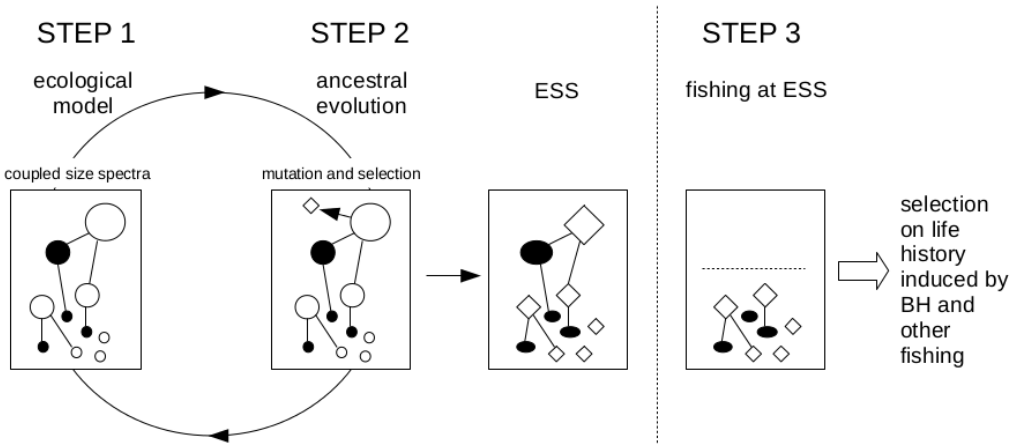

Figure 1: Road map of modelling steps. Boxes are cartoons of size spectra, with two species (filled and empty), and shapes depicting different phenotypes. The ecological model is run to determine the equilibrium state of the two species (STEP 1). New phenotypes are generated by mutation (STEP 2). The fate of a new phenotype is decided by the ecological dynamics (STEP 1). These steps are iterated as shown by the arrows until eventually the system reaches a state at which no further mutant can invade, an evolutionarily stable state (ESS). Contemporary fishing at this ancestral ESS generates new selection on the life history (STEP 3). The paper contrasts the strength of selection generated by balanced harvesting with size-at-entry and slot fishing.

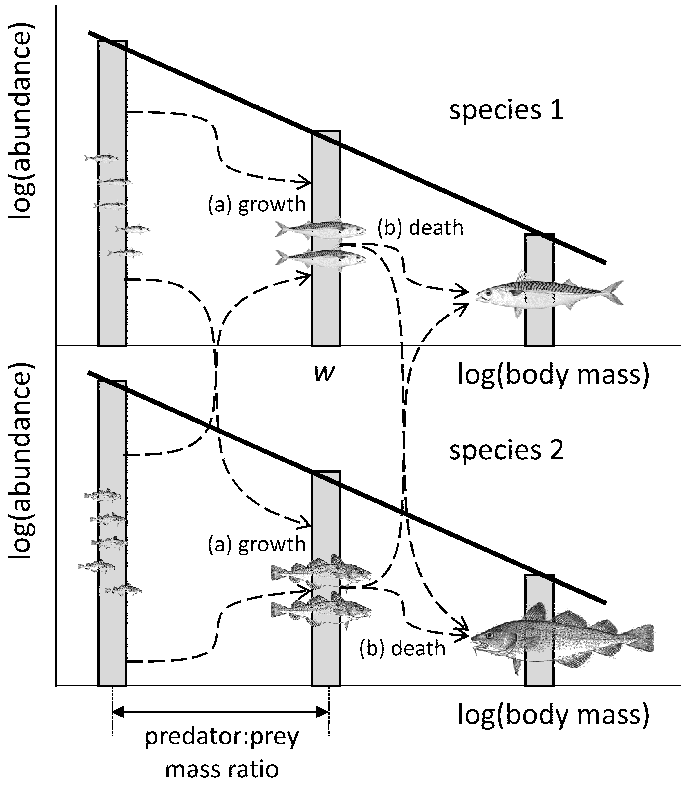

Figure 2: Processes acting on fish of body mass w. Growth comes from feeding on smaller fish of the same and other species, given by rate term (a) in Eq. (2.1). The main cause of death is predation and cannibalism by larger fish, a component of the rate term (b) in Eq. (2.1). Feeding is set by a preference function for prey relative to size w, determined by a species-specific predator:prey mass ratio. Heavy lines are examples of size spectra on log-log axes; these lines can change in shape over the course of time, as fish grow and die. Dashed lines show biomass flows from prey to predator.

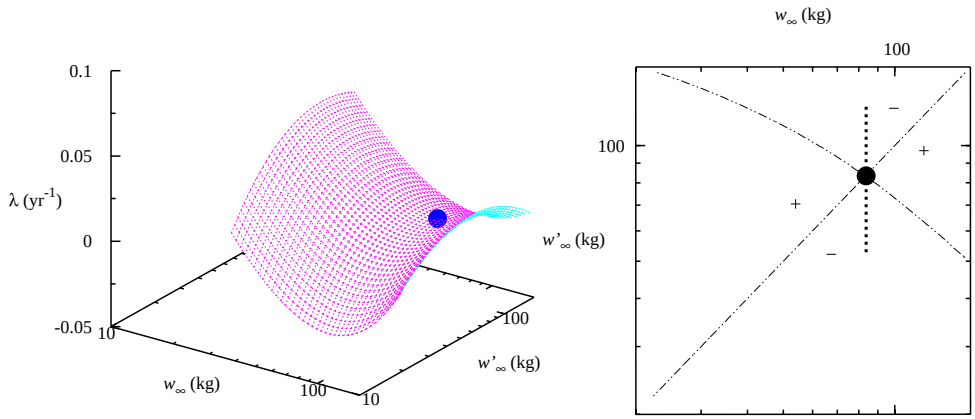

Figure 3: An example of an invasion fitness surface λ for a mutant with trait value w'_∞ as it enters a resident population with trait value w_∞, and its corresponding pairwise invasibility plot (PIP), the section through the surface at $\lambda = 0$. Filled circles mark the singular point of evolution, w^*_∞. Signs show the sectors of the PIP in which the invasion fitness of mutants is positive and negative, with boundaries given by the dash-dot line. The dotted line shows the direction in which selection gradient, Eq. (2.3), is measured.

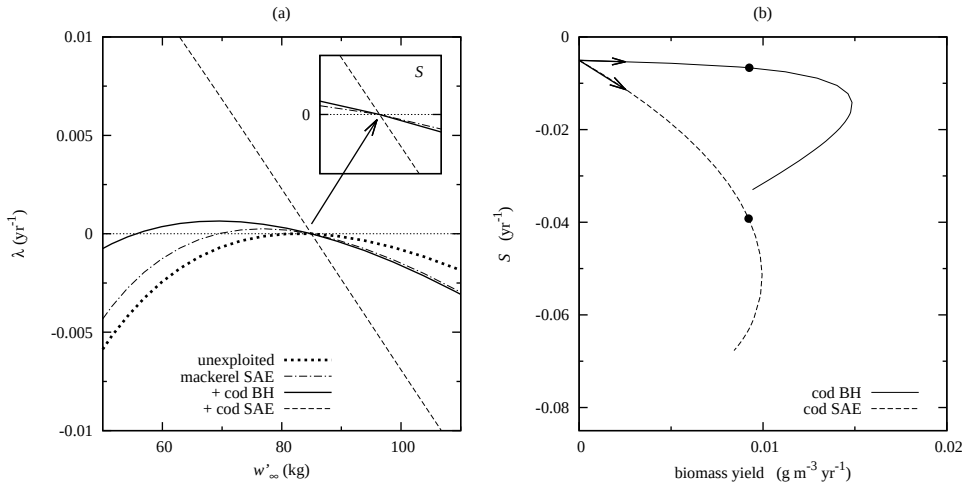

Figure 4: Invasion fitnesses and selection gradients S of cod mutants, under fishing schemes defined in the text. (a) Sections through invasion-fitness surfaces λ in the mutant direction w'_∞ at w^*_∞ (the direction of the dotted line in Fig. 3). The ancestral, unexploited system has a singular point of evolution w^*_∞ at 85 kg ($S = 0$). The selection gradient on cod from fishing is measured by the gradient S at w^*_∞, Eq. (2.3), as shown in the inset. A size-at-entry fishery (SAE) on mackerel, and no fishing on cod, leads to some selection on cod: S = -0.0051 yr^{-1}. Adding balanced harvesting (BH) on cod to the background fishing of mackerel, slightly increases selection on cod: S = -0.0067 yr^{-1} (cod minimum capture size 100 g, c = 11.0 m^3 g^{-1}). Adding size-at-entry (SAE) fishing on cod to the background fishing of mackerel, gives much stronger selection on cod: S = -0.0392 yr^{-1} (cod minimum capture size 1 kg, $F = 0.2$ yr^{-1}). (b) Effects of increasing cod fishing on selection gradients S and biomass yields (minimum capture sizes remain as in (a)). Arrows show the direction of increasing fishing on cod, starting from 0 and ending close to extinction of cod (near $c = 70$ m^3 kg^{-1} in the case of balanced harvesting, BH, and $F = 0.32$ yr^{-1} in the case of size-at-entry, SAE). Filled circles mark the selection gradients of the balanced and size-at-entry fisheries on cod, shown in panel (a).

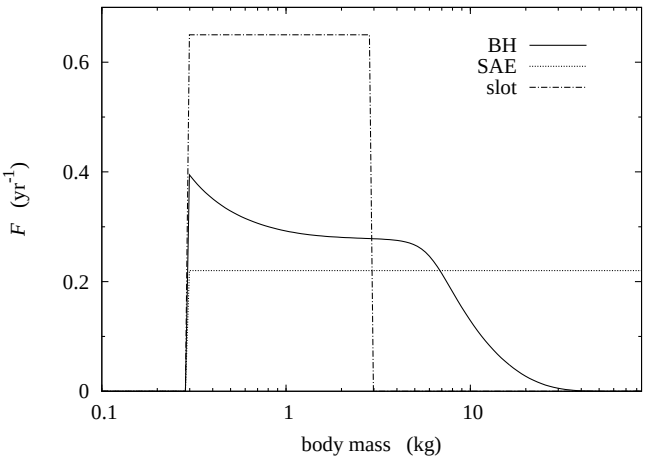

Figure 5: Three kinds of fishing mortality F: balanced harvesting (BH), size-at-entry (SAE), and slot. Each fishing pattern has a parameter controlling the overall fishing intensity, which moves the fishing mortality rates up or down; here their values are: BH $c = 30$ m^3 g^{-1}, SAE $F = 0.22$ yr^{-1}, slot $F = 0.65$ yr^{-1}. These parameter values were chosen to generate biomass yields near to 0.01 g m^{-3} yr^{-1} at steady state. They give selection gradients S (yr^{-1}): BH -0.008, SAE -0.045, slot -0.014.

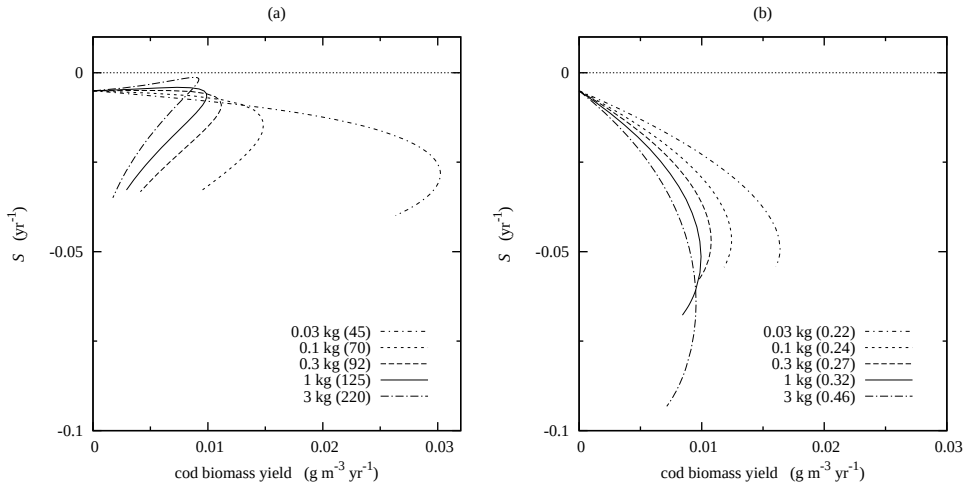

Figure 6: Selection gradients S and biomass yields of cod as fishing mortality on cod increases in: (a) balanced harvesting, and (b) size-at-entry fisheries. Each line describes a different minimum capture size, as given in the keys. Lines end where fishing mortality rate causes extinction of cod; this is close to the value given in brackets, c ($\mathrm{m}^3\ \mathrm{kg}^{-1}$) in the case of balanced harvesting, and F (yr^{-1}) in the case of size-at-entry fishing.

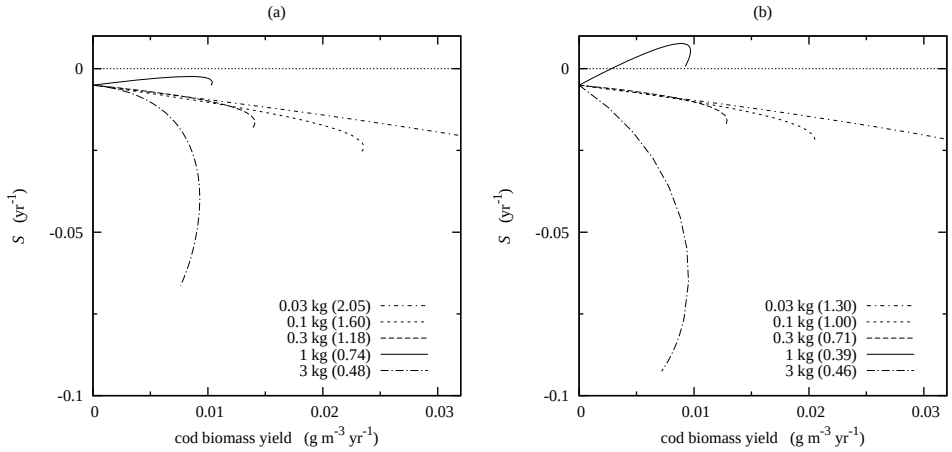

Figure 7: Selection gradients S and biomass yields of cod obtained as fishing mortality on cod increases in slot fisheries: (a) maximum capture size at 5 times the minimum; (b) maximum capture size at 10 times the minimum. Each line describes a different minimum capture size, as given in the keys. Lines end where fishing mortality rate F causes extinction of cod close to the value (yr^{-1}) given in brackets, except for minimum capture size 30 g, which is off the scale.

Appendices

A Multispecies dynamics

It is convenient to work in terms of the logarithmic body mass variable, $x = \ln(w/w_0)$, where w_0 is an arbitrary body mass. This gives a state variable $u_i(x,t)dx = \phi_i(w,t)dw$, with dimensions L^{-3}, which corresponds to the density of individuals of type i with log body mass in the range $[x, x+dx]$ at time t. 'Type' may be a species or a mutant within a species. The dynamics of $u_i(x)$ are given by the partial differential equation (Law et al., 2016):

$$\frac{\partial u_i}{\partial t} = \overbrace{-\frac{\partial}{\partial x}\left[\epsilon_i g_i u_i\right]}^{\text{growth}} + \overbrace{\frac{1}{2}\frac{\partial}{\partial x}\left[e^{-x}\frac{\partial}{\partial x}\left[\epsilon_i G_i u_i\right]\right]}^{\text{diffusion}} + \overbrace{\frac{b_i R_i}{2}e^{-x}}^{\text{reproduction}} - \overbrace{\mu_{\mathrm{tot},i}u_i}^{\text{mortality}}, \quad \text{(A.1)}$$

where the arguments x and t have been omitted from each function. The functions $g_i(x,t)$, $G_i(x,t)$ and $\mu_{\mathrm{tot},i}(x,t)$ respectively represent the rates of mass-specific prey biomass assimilation, diffusion and mortality for type i at log body mass x and time t. The function $R_i(t)$ is the reproduction rate (number of eggs produced per unit volume per unit time) of type i at time t. The function $\epsilon_i(x)$ is the proportion of assimilated prey biomass that is used for somatic growth by individuals of type i and log body mass x. Each of these functions will be defined below. The function $b_i(x)$ represents the mass distribution of eggs of type i. This is assumed to be a Dirac-delta function, corresponding to a unique log mass $x_{i,0}$ for type i. Eq. (A.1) is an extension of the size-based McKendrick–von Foerster equation to include a second-order diffusion-like term. This allows for demographic variability in size-at-age trajectories (Datta et al., 2010, 2011), although in practice this is small.

The model assumes that a predator of type i and log body mass x searches a volume of water $A_i e^{\alpha_i x}$ per unit time, and has a relative preference for prey that is given by a function $s_i(r)$ of the predator:prey mass ratio r. The relative encounter rate between individuals of type i and individuals of type j is denoted θ_{ij}. The mass-specific prey biomass assimilation rate $g_i(x)$ is calculated as an integral over the abundance of potential prey:

$$g_i(x) = A_i K e^{(\alpha_i - 1)x} \sum_{j=0}^{n} \theta_{ij} \int e^{x'} s_i(e^{x-x'}) u_j(x') dx'. \quad \text{(A.2)}$$

Similarly, the rate function for the second-order diffusion term $G_i(x)$ is

given by (Law et al., 2016)

$$G_i(x) = A_i K^2 e^{(\alpha_i - 1)x} \sum_{j=0}^{n} \theta_{ij} \int e^{2x'} s_i(e^{x-x'}) u_j(x') dx'. \tag{A.3}$$

Three sources of mortality are included: predation mortality, natural non-predation mortality (referred to as intrinsic mortality) and fishing mortality

$$\mu_{\mathrm{tot},i}(x) = \mu_i(x) + \mu_{o,i}(x) + \mu_{F,i}(x).$$

The predation mortality rate $\mu_i(x)$ is calculated as an integral over the abundance of potential predators:

$$\mu_i(x) = \sum_{j=1}^{n} A_j \theta_{ji} \int e^{\alpha_j x'} s_j(e^{x'-x}) u_j(x') dx'. \tag{A.4}$$

The intrinsic mortality rate $\mu_{o,i}(x)$ accounts for sources of mortality other than predation and fishing. We assume that this is proportional to the mass-specific needs for metabolism, relative to the mass-specific rate at which food becomes available at size x. These rates are set relative to their values at egg size, so $\mu_{o,i}(x_{i,0}) = \mu_{o,i}^{(0)}$ is a fixed baseline intrinsic mortality at birth for type i. The metabolic need should scale with body mass, and we write this as $\exp(-\xi(x - x_{i,0}))$, using the same exponent for all types. The mass-specific prey intake rate at size x relative to size $x_{i,0}$ is $g_i(x)/g_i(x_{i,0})$. Thus

$$\mu_{o,i}(x) = \mu_{o,i}^{(0)} \exp(-\xi(x - x_{i,0})) g_i(x_{i,0})/g_i(x), \tag{A.5}$$

which is also a function of time because it depends on the mass-specific prey intake rate $g_i(x)$.

The feeding kernel for type i is a Gaussian function of log predator-to-prey mass ratio r, with mean β_i and standard deviation σ_i. The feeding kernel is assumed to be 0 when $r < 1$ so that predators are always larger than their prey:

$$s_i(r) = \left\{ \begin{array}{ll} \frac{1}{\sigma\sqrt{2\pi}} \exp\left(-\frac{(\ln(r)-\beta_i)^2}{2\sigma_i^2}\right) & r \geq 1 \\ 0 & r < 1 \end{array} \right\}. \tag{A.6}$$

The function $\epsilon_i(x)$ the proportion of incoming prey biomass that is allocated to reproduction, using a form suggested by Hartvig et al. (2011):

$$1 - \epsilon_i(x) = [1 + \exp(-\rho_{i,m}(x - x_{i,m}))]^{-1} \exp(\rho(x - x_{i,\infty})). \tag{A.7}$$

Here $w_0 e^{x_{i,m}}$ is the body mass at which 50 % of the fish of type i are mature, and $\rho_{i,m}$ defines the body-mass range over which fish are maturing. The

asymptotic body mass $w_0 e^{x_{i,\infty}}$ is the size at which all incoming mass is allocated to reproduction and no further somatic growth is possible, the approach to this size being scaled by a parameter ρ common to all types.

The egg size $x_{i,0}$ and asymptotic size $x_{i,\infty}$ together give boundary conditions for Eq. (A.1), over which there is no flux of individuals. For simplicity, we do not deal with the dynamics of the plankton. This can be thought of as an assumption that the plankton operate on a short timescale relative to the fish community. The fixed plankton spectrum was taken as $u_0(x) = u_{0,0} \exp^{(1-\gamma)x}$, where $u_{0,0}$ is the abundance of plankton of mass 1 mg, giving a power-law relationship between body mass and abundance. Parameter values are given in Table 1.

B Invasion fitness

We consider a resident community consisting of two species coexisting at a stable equilibrium (though the following easily generalises to more than two species). The discretised version of the size-spectrum model consists of the abundance u_i of each species in size classes x_k ($k = 1, \ldots, N$) with step size Δx. The Jacobian matrix of the two-species system takes the form

$$\mathbf{J}_{\text{res}} = \begin{bmatrix} \mathbf{J}_{11} & \mathbf{J}_{12} \\ \mathbf{J}_{21} & \mathbf{J}_{22} \end{bmatrix}$$

where $\mathbf{J}_{ij}$ is the $N \times N$ matrix describing the dependence of species i on species j. We require that this two-species system has a stable equilibrium in which both species are non-zero, so that all eigenvalues of the Jacobian evaluated at this equilibrium, $\mathbf{J}^*_{\text{res}}$, have negative real part.

Now suppose the community is augmented by a mutant of species 2 indexed $2'$. The expanded system has a Jacobian matrix of the form

$$\mathbf{J}_{\text{aug}} = \begin{bmatrix} \mathbf{J}_{11} & \mathbf{J}_{12} & \mathbf{J}_{12'} \\ \mathbf{J}_{21} & \mathbf{J}_{22} & \mathbf{J}_{22'} \\ \mathbf{J}_{2'1} & \mathbf{J}_{2'2} & \mathbf{J}_{2'2'} \end{bmatrix}.$$

The state at which the resident species 1 and 2 are at the two-species equilibrium and the mutant $2'$ is absent is also an equilibrium of the augmented system. When the Jacobian matrix $\mathbf{J}_{\text{aug}}$ is evaluated at this equilibrium, the submatrices $\mathbf{J}_{2'1}$ and $\mathbf{J}_{2'2}$ are zero. Hence the Jacobian is

$$\mathbf{J}^*_{\text{aug}} = \begin{bmatrix} \mathbf{J}_{11} & \mathbf{J}_{12} & \mathbf{J}_{12'} \\ \mathbf{J}_{21} & \mathbf{J}_{22} & \mathbf{J}_{22'} \\ 0 & 0 & \mathbf{J}^*_{2'2'} \end{bmatrix} \tag{B.1}$$

The eigenvalues of this matrix consist of the eigenvalues of $\mathbf{J}^*_{\rm res}$, which all have negative real part, together with the eigenvalues of $\mathbf{J}^*_{2'2'}$, which is $\mathbf{J}_{2'2'}$ evaluated at the coexistence equilibrium of 1 and 2, with $2'$ at zero.

The elements of the Jacobian $\mathbf{J}_{2'2'}$ can be obtained from the partial differential equation Eq. (A.1) for the mutant, after discretization of log mass x. For brevity, we drop the mutant index by using u_k to denote $u_{2'}(x_k)$, and similarly g_k, G_k, ϵ_k, $\mu_{{\rm tot},k}$. The discretised version of the partial differential equation is then:

$$\begin{aligned}\frac{du_k}{dt} &= \frac{\epsilon_{k-1}g_{k-1}u_{k-1} - \epsilon_k g_k u_k}{\Delta x} \\ &\quad + e^{-x_k}\frac{\epsilon_{k-1}G_{k-1}u_{k-1} + \epsilon_{k+1}G_{k+1}u_{k+1} - 2\epsilon_k G_k u_k}{2\Delta x^2} \\ &\quad + e^{-x_k}\frac{\epsilon_{k-1}G_{k-1}u_{k-1} - \epsilon_k G_k u_k}{2\Delta x} \\ &\quad - \mu_{{\rm tot},k}u_k + \frac{\delta_{k1}Re^{-x_0}}{\Delta x},\end{aligned} \tag{B.2}$$

where δ_{kl} is the Kronecker-delta symbol.

From Eq. (B.2), the elements of $\mathbf{J}^*_{2'2'}$ are:

$$\begin{aligned}a_{kk} &= -\frac{\epsilon_k g_k}{\Delta x} - e^{-x_k}\epsilon_k G_k\left(\frac{1}{\Delta x^2} + \frac{1}{2\Delta x}\right) - \mu_{{\rm tot},k}, \\ a_{k,k-1} &= \frac{\epsilon_{k-1}g_{k-1}}{\Delta x} + e^{-x_k}\epsilon_{k-1}G_{k-1}\left(\frac{1}{2\Delta x^2} + \frac{1}{2\Delta x}\right), \\ a_{k,k+1} &= \frac{e^{-x_k}\epsilon_{k+1}G_{k+1}}{2\Delta x^2}, \\ a_{1k} &= \frac{e^{x_k - x_0}(1-\epsilon_k)g_k}{2}.\end{aligned} \tag{B.3}$$

All other elements of $\mathbf{J}^*_{2'2'}$ are zero because terms of the form $\partial/\partial u_l(g_k u_k)$ are all zero when evaluated at the equilibrium $u_k = 0$. The functions g_k, G_k and $\mu_{{\rm tot},k}$ depend on the resident abundances via Eqs. (A.2)–(A.4). In the special case considered in this model, where the only difference between the mutant $2'$ and the resident 2 is in its reproduction schedule (ϵ_k), the functions g_k, G_k and $\mu_{{\rm tot},k}$ will be identical to those for the resident 2. In other words, the mutant experiences the same size-dependent food intake and mortality rates as the resident, but differs in the proportion of incoming biomass that is allocated to reproduction. In the simpler case

of the McKendrick—von Foerster equation without diffusion, the Jacobian elements above omit all terms containing G_k.

The two-species coexistence equilibrium is stable to introduction of the mutant (i.e. a rare mutant will die out) if all eigenvalues of $\mathbf{J}^*_{2'2'}$ have negative real part. If $\mathbf{J}^*_{2'2'}$ has an eigenvalue with positive real part, the two-species equilibrium is unstable to the introduction of the mutant (i.e. a rare mutant will increase in abundance). The eigenvalue with largest real part λ is the rate of increase of the mutant population when the mutant is rare, i.e. the invasion fitness.

C Numerical methods

We took a community of two fish species, one growing to a small size, and the other to a large size, together with a fixed plankton spectrum. This was based on Law et al. (2016), the two species having parameter values motivated by mackerel and cod (Table 1) as described in Law et al. (2016). The dynamics were described by Eqns (A.1), with mackerel indexed $i = 1$, and cod $i = 2$. The asymptotic body mass of cod, $x_\infty = \ln(w_\infty/w_0)$, was set to evolve, and the mass at 50 % maturation, $x_m = \ln(w_m/w_0)$, evolved with it as fixed proportion $\ln(1/15)$ of this. The matrix of preferences θ_{ij} of predators of type i for prey of type j was:

$$\boldsymbol{\theta} = \begin{pmatrix} 0 & 0 & 0 & 0 \\ 1 & 1 & 0.2 & 0.2 \\ 1 & 0.2 & 1 & 1 \\ 1 & 0.2 & 1 & 1 \end{pmatrix}. \tag{C.1}$$

The first three rows of $\boldsymbol{\theta}$, indexed $i = 0, 1, 2$, refer respectively to: (0) plankton, (1) mackerel, and (2) cod with resident trait value x_∞. The final row refers to predation by mutant cod x'_∞, with predation preferences set to be the same as resident cod. The cross-species predation parameters, $\theta_{ij} = 0.2$, were chosen to take cod's x_∞ to a singular point of ancestral evolution x^*_∞ near that of the largest recorded cod.

TABLE 1 NEAR HERE

For numerical analysis, the continuous equations were discretized to a system of ordinary differential equations using as small a step size as practicable ($\Delta x = 0.05$). For given parameter values, we obtained a close approximation to the steady state from a numerical integration over a 100 yr time period, using a time step $\Delta t = 0.0005$, based on the Euler method. The Gaussian feeding kernel $s_i(r)$ Eq. (A.6) was truncated at $\pm 3\sigma$, and normalised to sum to 1. Fast Fourier transforms were used to compute

the convolution integrals. In cases where convergence to the steady state was slow, the time period of integration was extended. We terminated sequences of increasing fishing mortality at extinction of the cod.

Having reached the steady state of an arbitrary resident community (with cod's trait value at x_∞), we constructed the life history of a rare mutant with an altered trait value x'_∞. The Jacobian matrix of the resident community, augmented by the rare mutant, could then be built, with elements as given in Eqs (B.3). The invasion fitness, $\lambda(x'_\infty, x_\infty)$, of the mutant cod in the resident community is the real part of the leading eigenvalue of this matrix.

A singular point of evolution x^*_∞ occurs at

$$0 = \frac{\partial}{\partial x'_\infty}\lambda(x'_\infty, x_\infty)\big|_{x'_\infty = x_\infty}, \tag{C.2}$$

obtained numerically from a pairwise invasibility plot, using a grid of values (x'_∞, x_∞) of invasion fitness (Fig. 3). The strength of directional selection generated by fishing on cod at the singular point x^*_∞, was measured as

$$S = \frac{\lambda(x'_\infty + \delta x, x^*_\infty) - \lambda(x'_\infty - \delta x, x^*_\infty)}{2\Delta x}. \tag{C.3}$$

We checked the integrations by running two independently constructed versions of the code. We also checked the eigenvalue measure of invasion fitness by direct measurement of the rate of increase of rare mutants.

D Fishing mortality under balanced harvesting

Balanced harvesting, as defined in this paper, sets the fishing mortality rate on species i at time t in proportion to the current rate of somatic production at each body mass x, from some mininum capture size x_{min} onwards. Production rate is measured as

$$p_i(x,t) = \epsilon_i(x)\ g_i(x,t)\ u_i(x,t)\ w_0 e^x, \tag{D.1}$$

where $g_i(x,t)$ is the mass-specific assimilation rate of prey biomass Eq. (A.2), $\epsilon_i(x)$ is the proportion of this prey biomass allocated to somatic growth, $u_i(x,t)$ is the the density of individuals with log body mass in the range $[x, x+dx]$, and $w_0 e^x$ is the predator mass. This gives a fishing mortality rate $F_i(x,t)$

$$F_i(x,t) = \begin{cases} 0 & \text{if } x < \ x_{min} \\ cp_i(x,t) & \text{if } x >= x_{min} \end{cases}. \tag{D.2}$$

Here c is a constant of proportionality with dimensions vol. mass^{-1} or area mass^{-1}, and can be thought of as a mass-specific exploitation ratio. Production rate changes over time as the density functions $u_i(x,t)$ change. Balanced harvesting tracks the changing production rate until the ecosystem reaches its ecological steady state. The calculations in this paper use the fishing mortalities at this steady state.